International Journal of Reliability, Risk and Safety: Theory and Application

Online ISSN: 2676-3346

OPEN ACCESS

Vol. 7/ Issue 2/ Year 2024/ pp. 40-51
DOI: 10.22034/IJRRS.2024.7.2.4
Received: 05 August 2024, Revised: 18 September 2024, Accepted: 02 October 2024

Available online at: https://www.ijrrs.com

Case Study

Case Studies in Seismic Risk Assessment of Masonry Fire Station Buildings

Sasan Motaghed [1], Heshmatollah Mahmoodian [2] and Somayeh Dehdari [3]

1. Department of Civil Engineering, Faculty of Engineering, Behbahan Khatam Alanbia University of Technology, Behbahan, Iran

2 Center of Monitoring Assessment and Prediction of Natural Disasters (MAP), Behbahan Khatam Alanbia University of Technology, Behbahan, Iran

3. Faculty of Natural Resources, Behbahan Khatam Alanbia University of Technology, Behbahan, Iran

*** motaghed@bkatu.ac.ir**

Abstract

Risk analysis serves as a fundamental component for decision-making in pre-event planning aimed at crisis prevention and emergency management. This paper presents a comprehensive risk analysis for two fire station unreinforced masonry buildings as case studies. We conduct both deterministic (DSHA) and non-extensive probabilistic seismic hazard analyses (NEPSHA). The deterministic analysis indicates peak ground accelerations (PGA) of 0.6g and 0.33 at the building sites. The NEPSHA reveals PGA values corresponding to return periods of 10, 475, and 2475 years as 0.033g, 0.43g, and 0.745g, for site 1 and as 0.033g, 0.425g, and 0.761g, for site 2 respectively. Additionally, we establish fragility curves for the existing masonry buildings with median and low code grades. The analysis determines the probabilities of various damage levels at different hazard intensities, and utilizing FEMA's Hazus methodology, we estimate the debris generated. These results indicate that the unreinforced masonry building, despite being equipped with horizontal and vertical tie beams, fails to meet the seismic design requirements. Given the critical role of the fire department building in emergency response during and after an earthquake, further investigation into the building's performance under severe and deterministic (scenario) earthquakes is essential.

Keywords: Seismic hazard analysis; Petrochemical facilities; Fragility curve; Performance level; Loss estimation.

Nomenclature

APE	annual probability of exceedance
DSHA	deterministic seismic hazard analysis
ECDF	experimental cumulative distribution function
GIS	geographic information system
GMPE	ground motion prediction equations
GR	Gutenberg–Richter law
GRC	gas refinery company
IO	immediate occupancy
NEPSHA	non-extensive probabilistic seismic hazard analyses
PSHA	probabilistic seismic hazard analysis
PGA	peak ground acceleration
SCP	Sotolongo-costa and Posadas
UHS	uniform hazard spectrum
URM	unreinforced masonry

1. Instructions

Masonry structures are traditionally constructed using materials such as stone, brick, and concrete blocks [1,2]. These structures primarily serve as homes, particularly in towns and villages. In Iran, out of approximately 23 million residential units, nearly 10 million, or about 45%, are unreinforced masonry buildings [3]. However, they are also employed in the construction of essential facilities, including police stations, hospitals, and fire stations. According to the Iranian National Building Code, Part 8, (Third Edition)

How to cite this article:
S. motaghed, H. Mahmoodian, and S. Dehdari, "Case studies in seismic risk assessment of masonry fire station buildings," *International Journal of Reliability, Risk and Safety: Theory and Application*, vol. 7, no. 2, pp. 40-51, 2024, doi: 10.22034/IJRRS.2024.7.2.4.

masonry buildings are classified into two main categories [4]:

1. **Unreinforced Masonry Buildings** confined with concrete *tie* beam: These buildings are made with bricks, cement blocks, and stones, incorporating horizontal and vertical tie beams, typically of reinforced concrete, so that, the masonry walls bear gravity and lateral loads, tie beams enhance the overall integrity and ductility of the walls.
2. **Reinforced Masonry Buildings**: These buildings utilize cement blocks, bricks, stones, and reinforcing steel bars. In this configuration, the masonry components support compressive loads, and the steel reinforcement bears the tension loads and increases the structure's capacity to withstand lateral forces.

Considering the high number of unreinforced masonry structures, knowledge of their seismic behaviour and their condition after an earthquake is very important in providing seismic safety [5]. If masonry structures are used to build vital structures, considering the second-order effects of an earthquake - such as fire - checking their seismic condition becomes much more important [6]. From this perspective, the safety of essential masonry buildings-e.g. a fire station- against seismic hazards is a critical concern for engineers and managers. These buildings are essential for managing crises in the aftermath of earthquakes [7]. In the Bam earthquake the extensive destruction of essential structures such as hospitals, fire stations, governorates, municipalities, police stations, and other important buildings in Bam city was disastrous [8]. The fire department of this city was destroyed and all its personnel were killed or injured, as well as many equipment and facilities, including fire engines. The rescue service has fallen under the debris. The post-earthquake phase has faced a management crisis, and the experts recommend that all service, security, relief, and administrative buildings should be urgently restored to make crisis management possible [9,10].

These observations and similar reports show that risk analysis is a crucial step in managing potential threats and ensuring safety. The process involves several key components: hazard identification, vulnerability assessment, and exposure determination. The first step in risk analysis is to identify potential hazards that could lead to damage or harm. This includes recognizing factors that have the likelihood of causing adverse effects, such as natural disasters, accidents, or intentional acts [11,12].

Once the hazards have been identified, the next step is to evaluate the potential damages related to each hazard [13,14]. This involves assessing the vulnerability of the affected entities, such as people, property, or systems, to the identified hazards. Vulnerability analysis helps determine the extent to which an entity may be impacted by a particular hazard [15-18].

The final component of risk analysis is determining the consequences of the potential damages. This step involves assessing the likelihood and severity of the damages, as well as the potential impact on the affected entities. Exposure analysis helps identify the potential consequences of a hazard occurring and the extent to which it may affect the target population or area. Based on the results of the risk analysis, analysts can develop strategies to eliminate or control potential damages or consequences [19].

Given the significance of the issue, extensive seismic risk research has been conducted in the domain of masonry structures. Restrepo-Velez and Magenes presented a new procedure for assessing the seismic risk of unreinforced masonry buildings at an urban or regional scale. The key aspects of this approach are: formulating the structural capacity and response using mechanics-based concepts; representing seismic demand and structural capacity in terms of displacement; incorporating the most commonly recognized sources of uncertainty; and considering both in-plane and out-of-plane failure mechanisms. The procedure enables a comprehensive evaluation of seismic risk for Unreinforced Masonry Buildings by accounting for the mechanical properties, displacement-based assessment, uncertainty factors, and failure modes that are critical for this building typology, allowing for a robust estimation of seismic vulnerability at a large scale [20].

Snoj and Dolšek (2020) developed a methodology for seismic risk assessment and loss estimation for masonry buildings, based on pushover analysis. This approach allows for the estimation of losses using several performance metrics, including the exceedance probability of a specified economic loss, the expected annual loss, and the anticipated loss given a certain level of seismic intensity. The methodology facilitates the direct calculation of economic loss from structural analysis outcomes, integrating pushover analysis with incremental dynamic analysis of an equivalent single-degree-of-freedom model [21].

Traditionally, probabilistic seismic risk methods typically utilize a precise probabilistic model to assess the uncertainties associated with structural demand and capacity [22-24] and calculate the structural failure probability [25-27].

Some researchers have presented a loss estimation or fragility curve for masonry structures based on modelling [28] or by examining damage to masonry buildings in past earthquakes. D'Amato et al. (2022) presented typological loss curves and Expected Loss values based on the L'Aquila 2009 earthquake data. The proposed loss curves allow for an economic evaluation of the effectiveness of common local interventions, such as chains and ring beams, and their impact on reducing seismic risk [29].

Some nations have implemented Hazus, a standardized method created by FEMA, to assess potential losses from natural hazards like earthquakes [30]. Hazus combines engineering principles and mathematical models based on Geographic Information Systems (GIS) to evaluate both structural and non-structural damages, as well as the associated economic and social impacts.

Some countries have adopted Hazus, a standardized methodology developed by the FEMA, for determining the potential losses of natural hazards, such as earthquakes [33]. Hazus integrates engineering science and mathematical models based on GIS to estimate structural and nonstructural damages and their resulting economic and social losses. This method has been used for seismic risk analysis of bridges [21], cities [32-33], and reinforced concrete structures [34].

The current paper focuses on the seismic risk assessment of two cases of unreinforced masonry buildings. The first case is located on a petrochemical site and serves as a fire-fighting facility. This building houses both personnel and equipment. The second case is a part of the fire station in Behbahan city. A deterministic and non-extensive probabilistic seismic hazard analysis (NEPSHA) has been conducted [33] for seismic hazard determination. Then we use the general fragility curves for loss estimating. Based on the observed damages, the amount of debris generated and potential casualties have been estimated. The goal of this study is to assess the resilience and performance of reinforced masonry systems. By understanding how masonry behaves under seismic conditions, engineers can develop improved design methodologies and construction practices to enhance the safety and survivability of buildings in the events.

2. Methodology

As mentioned in the previous section, risk analysis involves identifying the potential consequences of an event. It comprises three key components: hazard, vulnerability, and exposure, as illustrated in Figure 1. This process ultimately aims to assess the likelihood of the various outcomes associated with the identified hazard.

In this way, to calculate the seismic risk it is necessary to determine the seismic hazard, determine the vulnerability of the building (fragility curve) and examine the consequences of the damage to the building (exposure). For more clarity, these items are also given in Figure 1. Based on the type of the intended damage, the third part of the diagram can include different items. In this paper, the volume of debris and the number of casualties is considered.

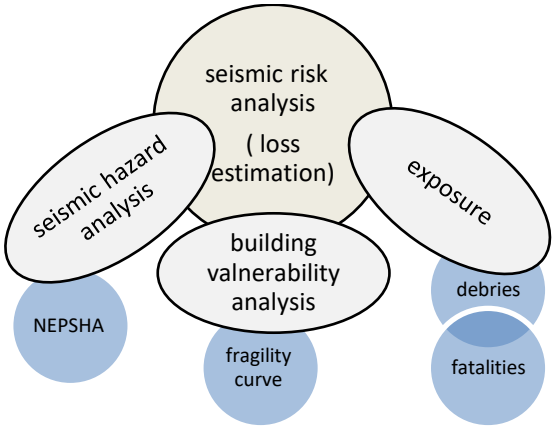

Figure 1. Seismic risk components

The initial phase of risk analysis involves conducting a hazard analysis [34-35]. Earthquake hazard analysis can be conducted using two main approaches: deterministic and probabilistic. The deterministic seismic hazard analysis (DSHA) method relies on specific earthquake scenarios, while the probabilistic seismic hazard analysis (PSHA) considers the likelihood of different earthquake magnitudes occurring. In this study, we employ a combination of the deterministic approach and a specific type of probabilistic analysis called Non-extensive Probabilistic Seismic Hazard Analysis (NEPSHA).

In the NEPSHA procedure, analogous to the traditional PSHA approach, the mean annual rate at which a specific threshold value, x, of a ground motion intensity measure (IM) is exceeded, can be calculated using the equation developed by Cornell in 1968 (Cornell, 1968).

$$\lambda_{IM}(x)=\sum_{i=1}^{n_{flt}} \upsilon \iint_{mr} G_{IM|M,R}(IM\geq x|m,r) f_M(m) f_{R|M}(r|m)\,dm\,dr \qquad (1)$$

Where n_{flt} refers to the number of causative faults, ν indicates the average annual frequency of earthquakes with magnitudes falling between a specified lower threshold, m_{min}, and an upper threshold, m_{max}. *M* and *R* represent the moment magnitude of the earthquake and the distance from the source to the site, respectively. $G_{IM|M,R}$ denotes the probability that an intensity measure (IM) surpasses a value of *x*, given that an earthquake of magnitude *m* occurs at a distance R. This probability can be determined using ground motion prediction equations (GMPE). f_M signifies the probability density function (PDF) of the earthquake magnitude and $f_{R|M}$ is the PDF of distance *r* conditional on *m*.

NEPSHA differs from traditional PSHA in its approach to modelling earthquake recurrence (f_M) [36]. The PSHA is modelled using Gutenberg–Richter (GR) law [37] while in the NEPSHA the f_M is stated based on the SCP model as:

$$f_M(m) = \frac{\left[1+a_{SCP}(q-1)(2-q)^{\frac{1-q}{q-2}}\times 10^{2m}\right]^{\frac{1}{1-q}} \times a_{SCP}(2-q)^{\frac{-1}{q-2}} \times 2\times 10^{2m}\ln 10}{\left[1+a_{SCP}(q-1)(2-q)^{\frac{1-q}{q-2}}\times 10^{2m_{min}}\right]^{\frac{2-q}{1-q}} - \left[1+a_{SCP}(q-1)(2-q)^{\frac{1-q}{q-2}}\times 10^{2m_{max}}\right]^{\frac{2-q}{1-q}}} \quad (2)$$

$$; m_{min} < m < m_{max},$$

This doubly truncated magnitude distribution can be termed a bounded SCP recurrence law.

The appropriateness of this relationship can be evaluated by its compliance with regional data.

The next phase of risk analysis involves evaluating the vulnerability of the structure. Due to variations in national design codes, construction practices, and building materials across regions, it is common practice to develop general fragility functions for the different types of common buildings in each area [38-39]. Karim Zadeh et al. classified typical Iranian buildings into 35 categories based on materials, load-bearing system, age, height, and code compliance level. These generalized fragility curves are very useful for assessing approximate vulnerability and examining large areas. They considered four damage criteria corresponding to minor, moderate, extensive, and complete damage levels. These limit states were defined based on the yield and ultimate displacement of the system [40].

Different performance levels of the structure can be assessed based on its damage limit status. Figure 2 intuitively illustrates the connection between the damage limit status and the corresponding performance levels [38].

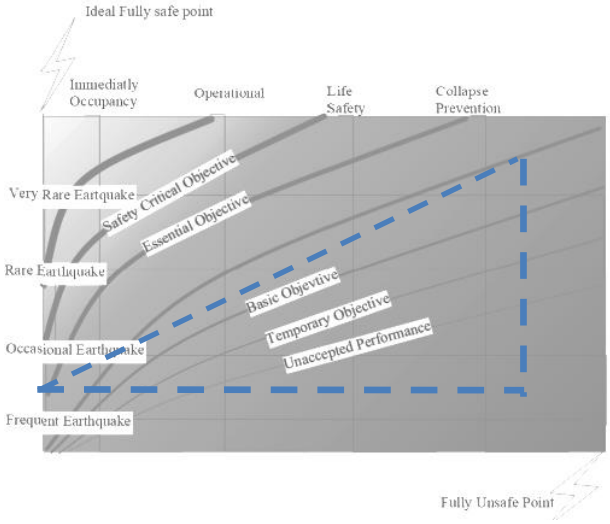

Figure 2. Relationship between performance levels and structural damage levels in different earthquake levels

Using the above data, it is possible to assess how a structure would perform during an earthquake. Building codes often include guidance tables to assist with this analysis. An example of such a table is shown in Figure 2.

Figure 2 provides a new presentation of the combination of the concepts of seismicity (earthquake hazard), vulnerability and building objective performance (earthquake risk). The ordinate shows the seismic hazard. As you move up, the seismic hazard increases. The highest point of the ordinate indicates an earthquake with a very low probability of occurrence and a very high hazard.

The abscissa of Figure 2 shows the performance of the building. By moving to the right, the performance of the building weakens. That is, the more the performance moves to the right, the lower the safety of the building in earthquakes.

In this way, the safest building is placed in the upper left corner (Ideal fully safe point) and the most unsafe building is placed in the lower right corner (fully unsafe point) of the scheme.

The curves placed inside the figure show the defined goals of the ordinary building's codes (e.g. ATC/SEAOC, Code No. 360 etc.). Positioning a curve in the upper left indicates a greater safety target. The famous curves that have specific definitions in the rehabilitation and retrofit regulations are shown with their names. As seen in Figure 2, according to the regulations, the "Basic Objective" is the minimum acceptable limit for buildings. In this way, it can be roughly said that the performance of the building in an earthquake should not be placed in the lower right triangle (shown by dashed lines) [41].

By evaluating the expected damage and performance of the building, the Hazus method can be employed to estimate the amount of debris that would result and potential casualties. To utilize this approach, two key pieces of information are required:

1. The unit weight (weight per unit area) of the building materials can be found in Table 1. According to the data provided in Table 1, the weight per square meter of the building material is 976 kilograms. If the actual load or existing load of the building differs from this specified weight, the values listed in Table 1 can be adjusted accordingly to reflect the accurate weight per square meter for the building.
2. The anticipated volume of debris is provided in Table 2. According to Table 2, for example, in minor building damage, 5% of structural Break and wood and 2% of non-structural Break and wood are destroyed. In this case, the amount of structural and non-structural Reinforced concrete and steel is zero. In this way, based on the information in Tables 1 and 2, we have

$$0.05 \times 442 + 0.02 \times 43 + 0 \times 337 + 0 * 114 = 22.96 \text{ kg}/m^2$$

Therefore, the volume of the total debris in the unit area is equal to 22.96 kg/m^2, which in this case consists of break and wood. To calculate the total volume of debris, this number must be multiplied by the area of the building.

With these inputs, the Hazus methodology can generate projections for debris accumulation and human impact following an earthquake event, based on the known characteristics and performance of the structure.

Table 1. Unit weight (kg/m2) for unreinforced masonry building [35]

Reinforced concrete and steel			Break, wood, and others		
Non-Structural	Structural	sum	Non-Structural	Structural	sum
43	442	485	114	377	491

Table 2 The debris produced from the damaged structural and non-structural parts (in percent weight) for unreinforced masonry building [35]

Debries type		Debries percent	
		Break and wood	Reinforced concrete and steel
Structural damages	minor	5	0
	moderate	25	2
	extensive	55	25
	Complete	100	100
Non-Structural damages	minor	2	0
	moderate	12	10
	extensive	45	29
	Complete	100	100

The probability of debris can be determined by multiplying the probability of damage (as outlined in the procedure), the unit weight (refer to Table 1), and the percentage of debris (see Table 2), as follows:
probability of debris = probability of damage × unit weight ×percentage of debris

The unit weight indicates the weight of materials for each unit area of the building.

3. Seismic hazard analysis

The building for the study is situated within the Gas Refinery Company (GRC). According to the active faults map (Figure 3), the GRC is positioned in a seismic zone. Additionally, the earthquake survey for the area indicates significant seismic activity in the region. The primary faults relevant to this area are detailed in Table 3.

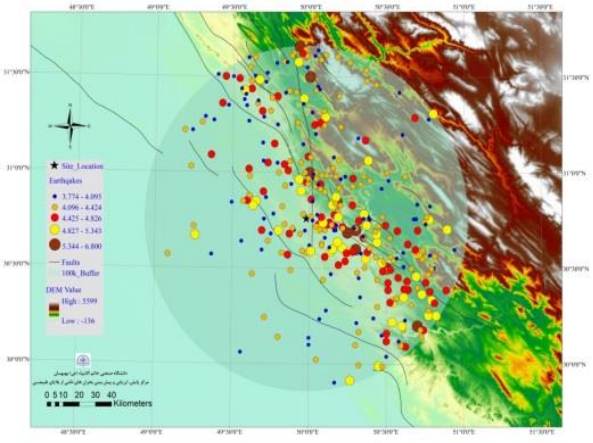

Figure 3. Active faults and earthquake epicenters around the GRC

Based on this visual data, the subsequent hazard analysis will be conducted using both deterministic and probabilistic approaches.

To perform DSHA, information on faults and the ground motion prediction equations (GMPE) are needed. Faults information, including the maximum magnitude (M_{max}) and distance (R), are given in Table 3.

Table 3. Faults and Fracture lineament around GRC and Behbahan city

fault	M_{max}	Length (km)	Nearest Distance to site 1 (km)	Nearest Distance to site 2 (km)
Behbahan	7.35	78.8	8.4	17.8
Tashan	7.26	65.2	11.0	20
Izeh	7.77	192.7	21.1	3.6
Aghajari	7.52	113.1	23.7	19.9
Baba Khaneh	6.69	19.3	24.0	39.2
Mishan	7.40	87.2	28.7	42.5
Rag Sefid	7.52	113.5	44.7	28.2
Ramhormoz	7.87	237.2	49.4	71.1
M. F. F	7.44	95.9	71.2	92.5
Lahbari	7.89	249.0	76.1	96.2
M.F	6.69	19.4	81.8	99.8
Kuh-e Noh	6.80	24.6	82.0	97.6
Maroon	6.86	27.7	90.3	89.6
Sivak	7.09	45.4	94.4	105.9
M.F	6.71	20.1	97.6	108.6
Jarreh	6.93	32.4	100.3	120.1
Seh Paran	6.58	15.3	102.4	121.7
Mangasht	6.73	21.3	109.5	129.8
Shah Neshin	6.86	27.6	109.5	130.1
Dena	7.48	104.4	112.9	101.2
Mordehfel	7.13	49.9	115.5	110.2
Cheshmeh Chenar	6.71	20.2	122.1	115.6
Sarakan-e Bala	6.72	20.8	123.2	118.2
Massan	7.38	83.7	124.0	101.5
Kazerun	7.56	123.2	124.4	101.3
Bazoft	7.04	40.9	125.8	141.2
Ahvaz	7.51	110.7	126.7	145.8
Kermani	7.00	37.6	127.3	144.2
noname	7.08	44.6	127.3	147.8
Chal Kalagh	7.09	45.8	130.5	138.7
Ab-e Rak	6.61	16.6	133.5	128.4
Dopolan	7.25	64.0	134.8	120.1
Kuh Siah	7.31	71.7	135.1	120.7
Bideh	6.94	33.2	135.3	119.5
Sabzeh Kuh	7.18	54.7	137.7	152.3
Ahvaz	6.61	16.3	138.8	151.7
Taveh Siah	6.65	17.9	139.0	158.9
Farum	6.57	15.0	140.5	150.2
Kordan	6.96	34.2	141.5	135.2
Borazjan	7.76	185.9	143.0	129.9
Avafi	6.57	15.1	147.6	164.8
Kakan	6.70	20.0	149.1	158.7
M.F	6.93	32.7	149.4	158.4
Mourchegan	6.91	31.1	149.7	161.5
H. Z	7.37	82.2	151.5	168.5
Semirom	6.90	30.1	152.5	152.5
Ardal	7.78	195.4	153.7	168.9
noname	7.22	59.8	154.5	154.1
Masjed Soleiman	6.95	33.7	158.6	160.2
Janga	6.94	33.1	159.2	162.4
Hana	6.80	24.7	159.6	162.5
Zard Kuh	7.85	227.5	160.8	161
Kuhe-eAqdagh	6.88	29.1	161.0	160.3
M.Z.R	7.54	119.0	161.0	161.5
M.Z.R	7.04	40.8	163.2	162.4
Mafarun	7.32	74.2	163.5	167.8

fault	M_{max}	Length (km)	Nearest Distance to site 1 (km)	Nearest Distance to site 2 (km)
M.Z.R	7.10	46.4	168.3	170.8
M.Z.R	7.80	204.3	168.9	170.9
Andakan	7.18	54.5	173.4	175.8
Solaghan	7.60	132.9	180.1	185.7
Karehbas	7.56	122.7	180.3	179.8
noname	6.39	10.3	181.6	182.6
Dasht-e Gol	6.71	20.3	182.7	185.2
Qalat	7.08	44.6	184.2	184.1
Shahr-e Kord	7.67	154.2	185.8	186.7
Susan	6.69	19.5	185.9	189.5
Kelestan	7.14	50.4	187.1	196.8
M.F	7.44	96.0	187.7	>200
noname	6.70	20.0	187.9	>200
Chal-e Munar	6.60	16.1	193.4	>200
Katah	7.45	96.8	193.6	>200
Cher cher	6.95	33.6	198.2	>200
Z. F. F	7.61	136.2	199.2	>200

The ruptures of the Behbahan, Tashan, Aghajari, and Izeh faults are classified as scenarios for Deterministic Seismic Hazard Analysis (DSHA). Details of these faults are presented in Table 3. Ghasemi et al. (2009) developed an empirical spectral ground-motion prediction equation for 5%-damped horizontal spectral acceleration applicable to Iran. The model was derived using Iranian accelerogram data supplemented with selected West Eurasian records to cover a wider range of magnitude and distance. The functional form of the relationship is:

$$\mathrm{Log}_{10}\,\mathrm{Sa} = a_1 + a_2 M + a_3 \log_{10}(R + a_4 10^{\,a5M}) + a_6 S_1 + a_7 S_2$$

Where the a1 to a5 and S_1 and S_2 parameters for 17 periods are given in Ghasemi et al., 2009 [42]. The values of R and M are given in Table 3 for the considered sites. The model is applicable for magnitudes mostly in the range of 5.0-7.4 Mw and rupture distances (R_{rup}) and hypocentral distances (R_{hyp}).

According to the DSHA analysis, the uniform hazard spectrum (UHS) for four faults located near the sites are calculated and shown in Figure 4 and Figure 5 for site 1 and site 2 respectively. The findings indicate that the Izeh fault poses the greatest hazard to Site 1 due to its proximity to the site. This fault, which stretches approximately 200 km, has the potential to generate an earthquake with a magnitude of around 7.73 Mw. Such an earthquake could result in peak ground acceleration (PGA) of 0.6g at the site, which is nearly double the standard PGA value of standard No.2800 for the area. Other faults in the vicinity yield PGAs that are closer to the standard No. 2800 value. The reason for this observation is that the site is near fault.

In site 2, the hazard is near the limits of standard No. 2800. The reason is that this site is far from fault.

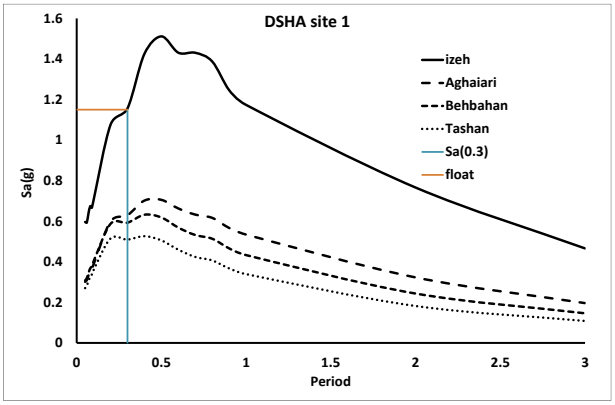

Figure 4. Uniform hazard spectra (UHS) in site 1 using DSHA

To perform a probabilistic seismic hazard analysis, it is necessary to determine the parameters of the earthquake recurrence law, also known as seismicity parameters. Two commonly used models for calculating these parameters are the Gutenberg-Richter (GR) model and the Sotolongo-Costa and Posadas (SCP) model.

Before proceeding with the analysis, it is crucial to evaluate which of these two models is better suited for the region. The suitability can be determined by fitting both models to the regional seismicity data (ECDF or experimental cumulative distribution function) and comparing the results, as shown in Figure 6. The figure illustrates that the SCP relationship aligns more closely with the seismicity data. The parameters for the SCP model are set at $a = 1.53 \times 10^{-7}$ and q = 1.608. Now we proceed with NEPSHA.

Based on the NEPSHA, seismic hazard values for three different annual probabilities of exceedance (APE) levels (0.1, 0.0021, and 0.0004) have been calculated using the Open Quick software. The tapered minimum magnitude is 4.5-5.5 [43] and the maximum magnitude is selected based on Table 3. In NEPSHA, the GMPEs of Akkar and Kagnan 2020 (0.2), Akkar et al. 2014 (0.35), Chiu and Yangs 2008 (0.35), and Zhao et al. (2006) (0.1) have been used [44-47]. The numbers in parentheses indicate the weight of each relation in combining the results using the logic tree. The NEPSHA results are shown in Figure 7 and Figure 8 for Site 1 and Site 2 respectively.

For site 1, The earthquake PGA values are 0.03 g for 10 years (99.5% probability of exceedance in 50 years), 0.42 g for 475 years (10% probability of exceedance in 50 years), and 0.74 g for 2475 years (2% probability of exceedance in 50 years) return periods. When compared to standard No.2800, which sets the threshold at 0.3 g for a 10% probability of exceedance in 50 years, it is evident that this area exceeds the standard requirements.

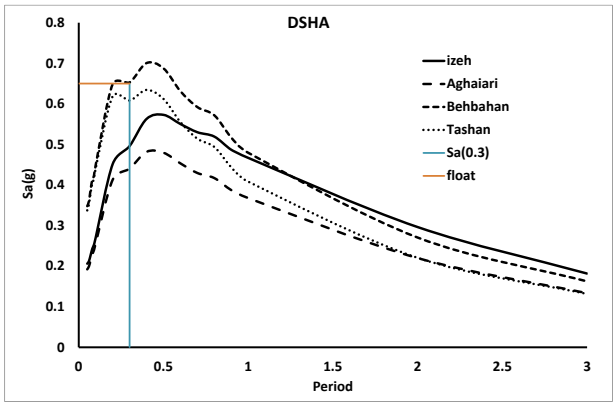

Figure 5. Uniform hazard spectra (UHS) in site 2 using DSHA

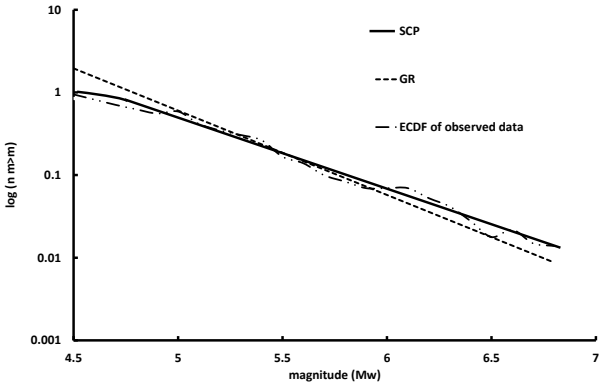

Figure 6. Comparison of ECDF observed data with the GR and SCP models

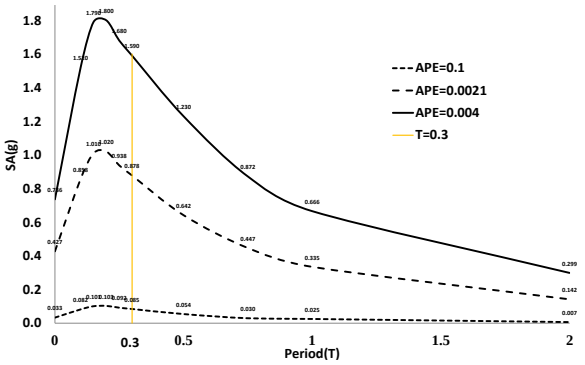

Figure 7. Uniform hazard spectra (UHS) of severe, design and service earthquakes in site 1 based on NEPSHA

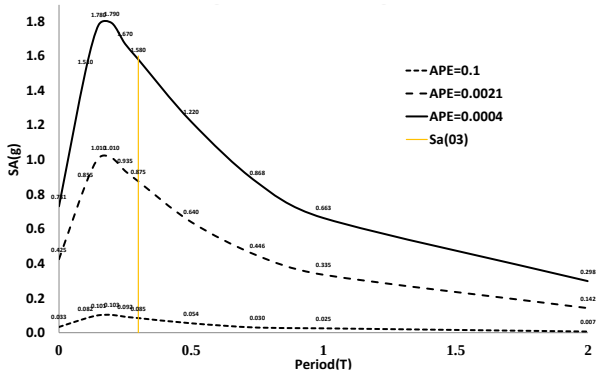

Figure 8. Uniform hazard spectra (UHS) of severe, design and service earthquakes in site 2 (in Behbahan city) based on NEPSHA

For site 2, the earthquake PGAs are 0.03g for 10 years, 0.42g for 475 years, and 0.74g for 2475-year return periods. The PGA of standard No.2800 is 0.3 g for a 10% probability of exceedance in 50 years.

Based on the fragility curve requirements [40], the value of SA (0.3) should be extracted from these curves for the next step.

4. Building information, fragility, and seismic risk

Case 1: the two-story structure is situated at the geographic coordinates of 30.75949 N and 49.97785 E. It is a masonry building with 160 square meters area and standing 4.5 meters tall. Constructed in 2006, the building assigned to average code and is classified as a regular building. The building's layout and elevation are illustrated in Figure 10-2. The key question is whether the placement criteria for this building have been fulfilled, given its significance following the earthquake [48-50]. Due to its location underneath the shed, the two-story building is not visible in this photograph. The layout, elevation view and location of the building are shown in Figures 9 and 10 respectively.

a

b

Figure 9. (a) Layout and **(b)** elevations of building 1

The fragility curve is a graph that shows the probability of a certain level of damage in the structure as

a function of the intensity of ground motion (for example, spectral acceleration or maximum ground acceleration). This curve is useful for predicting the probability of damage in a specific structure under different levels of ground motion.

Figure 15 shows the fragility curves of the structure. The fragility curves show the probability distribution of different damage intensities in the four performance levels of the structure, which include minor, moderate, extensive, and complete damage.

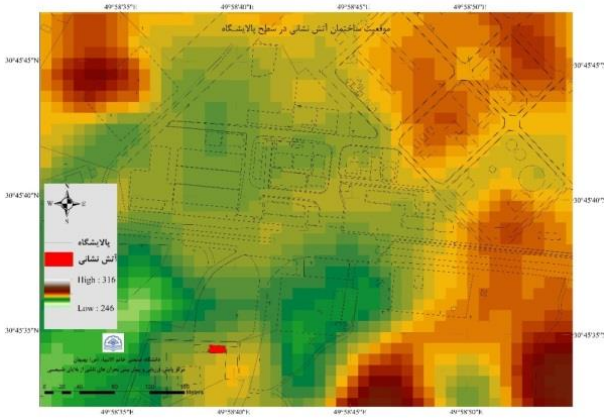

Figure 10. Location of the Site1 in the GRC

Case 2: A one-story structure is situated at the geographic coordinates of 30.58564 N and 50.23470 E. It is a masonry building with 120 square meters area and stands 3 meters tall. Constructed in pre pre-standard era, the building was assigned to low code. The building's location and elevations are illustrated in Figure 11.

a

b

Figure 11. (a) Layout and **(b)** elevations of building 2

Figure 12 shows the fragility curves of the building 1. The fragility curves show the probability distribution of different damage intensities in the four performance levels of the structure, which include minor, moderate, extensive, and complete damage.

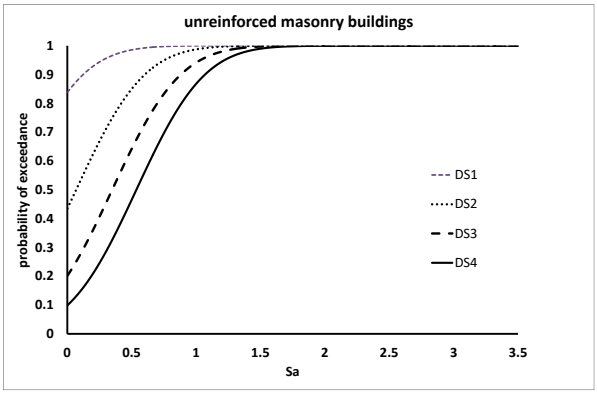

Figure 12. Fragility curves for different damage statuses (minor, moderate, extensive, and complete) for building 1

Figure 13 shows the fragility curve of Building 2. According to Figure 12, for the spectral acceleration above 1.5g, the probabilities of all types of damages in the building are 100%. For building 2, the 100% probability of total damage occurs at a much lower spectral acceleration (about 0.8g). This shows that building number 2 is very weak.

Now, with the seismic hazard and the fragility curve, the probability of damage can be calculated for each level of damage. The amount of damage calculated for Building 1 and Building 2 is given in Table 4 and Table 5.

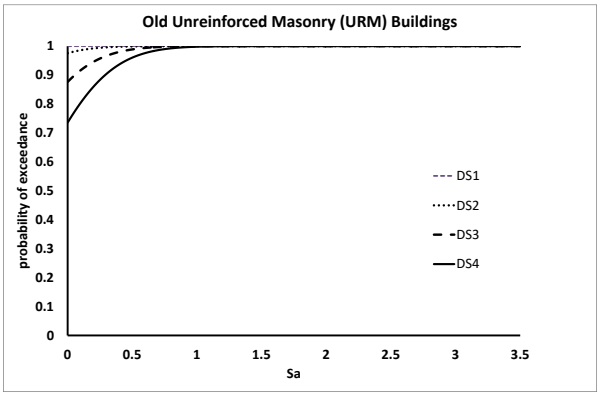

Figure 13. Fragility curves for different damage statuses (minor, moderate, extensive, and complete) for building 2

Table 4. Probability of exceeding different levels of damage in deterministic, severe, design, and service earthquakes at the building1

hazard	Performance level			
	LS1	LS2	LS3	LS4
Deterministic	100	100	99.5	97
APE=0.004	100	100	100	100
APE=0.021	100	99	95	88.5
APE=0.1	94	66	38.5	23

Table 5. Probability of exceeding different levels of damage in deterministic, severe, design, and service earthquakes at Building 2

hazard	Performance level			
	LS1	LS2	LS3	LS4
Deterministic	100	100	100	99.5
APE=0.004	100	100	100	100
APE=0.021	100	100	100	96.5
APE=0.1	99	90.5	75	65

Based on Table 4, it is probable that Building 1 will incur extensive damage during the design earthquake. In the case of deterministic and severe earthquakes, the probability of moderate damage rises to nearly 100%.

Table 5 shows that in building 2, the situation is more critical, and in the design earthquake, the damage is almost 100%. Even in a service earthquake, the probability of damage is over 50%.

Now having the damage probabilities, we can estimate the amount of debris and casualties using the Hazus method. This involves calculating debris volume based on the weight of materials per square area (see Table 1), the debris generated from damaged structures (refer to Table 2), and the unit weights of the debris.

In building 1, in the event of a severe earthquake, approximately 90.5 tons of debris is expected from this building, which would result in 10% of the road being closed. Fortunately, this would not significantly disrupt vehicle traffic. For deterministic, design, and service earthquakes, the estimated debris amounts are 83.124 tons, 82.86 tons, and 29.93 tons, respectively, with corresponding casualty figures of 2.56, 0.43, and 0.08 fatalities. Given that there are 7 people in building 1, we anticipate around 3.2 casualties during a severe earthquake, with approximately 1.5 individuals likely to be trapped. During night time, when only 3 people are present in the building, it is estimated that 1 person may sustain injuries in the event of a design earthquake.

In Building 2, in a severe earthquake, approximately 90.5 tons of debris is expected, which would lead to the closure of 10% of the road. Fortunately, this would not cause significant disruptions to vehicle traffic. For deterministic, design, and service earthquakes, the projected debris amounts are 83.124 tons, 82.86 tons, and 29.93 tons, respectively, with estimated casualty figures of 2.56, 0.43, and 0.08 fatalities. Considering there are 7 individuals in building 2, we predict around 3.2 casualties during a severe earthquake, with about 1.5 individuals likely to be trapped. At night, when only 3 people are in the building, it is estimated that 1 person may incur injuries during a design earthquake.

These results show that the use of masonry structures is not suitable for the construction of critical structures in areas with moderate and high seismicity.

In the end, it is noted that the results of this study are based on assumptions, each of which is associated with uncertainties. The most important uncertainties are as follows:

- Characteristics of faults include length, location and seismic characteristics.
- Seismicity model and parameters caused by inconsistency of model with data, insufficient data and missing historical and instrumental data.
- Uncertainty due to the choice of GMPE.
- Uncertainty caused by the choice of fragility curve due to the spread of masonry structures in Iran the lack of specific standards at the time of construction of most of these structures and the changes in labour laws and relations.
- Uncertainty caused by the use of debris volume and loss assumptions of global regulations.

In this way, the results of this study, like other studies based on models, are associated with uncertainty, which must be considered in applying and interpreting the results.

5. Conclusion

Earthquakes can be the initiator of many secondary accidents such as fire, landslide, and liquefaction. Among these, fire is one of the most important secondary hazards after earthquakes. In some cases, due to incendiary sources such as wood, gas and electricity, fire in urban or rural areas can cause much more severe damage than an earthquake.

Due to the increasing importance of providing safety services and measures to prevent catastrophic secondary effects in cities, fire stations have found a very important role in crisis management. Undoubtedly, the real tie timely service of fire stations is critical in this condition.

Masonry structures are extensively utilized in construction across Iran. While these structures are predominantly employed for residential buildings, they are also observed in critical facilities, including essential infrastructure. A notable example is the fire department building at a petrochemical facility. This paper aims to explore whether masonry building is a viable option for critical structures or not. The investigation focuses on a specific structure built in 2006 within a gas refinery. To address this inquiry, a comprehensive earthquake risk analysis has been conducted, employing both deterministic and non-extensive probabilistic hazard assessments, fragility curve extraction, and damage evaluations using suitable methodologies. Results indicate a significantly high probability of severe damage to the building during an earthquake. The structure will likely experience extensive damage during the design earthquake scenario. In cases of deterministic and severe earthquakes, the likelihood of moderate damage approaches 100%. Therefore, in regions with relatively high seismic hazards, it is crucial to emphasize seismic design considerations, particularly at the immediate occupancy (IO) performance level.

The findings of this research show that masonry buildings do not meet the needs of vital structures, even with compliance with seismic regulations. For this

reason, it is necessary to apply more restrictions on the use of masonry structures for essential buildings. For this purpose, applying additional requirements for such buildings can be considered.

Acknowledgements

We thank Bid-bland Gas Refinery Company for supporting the research. Also, we thank the Center for Monitoring Assessment and Prediction of Natural Disasters (MAP) of Behbahan Khatam Alanbia University of Technology.

Conflict of Interests

No conflict of interest has been expressed by the authors.

6. References

[1] R. K. Mazumder, S. Rana, and A. M. Salman, "First level seismic risk assessment of old unreinforced masonry (URM) using fuzzy synthetic evaluation," *Journal of Building Engineering*, vol. 44, 2021, Art. no. 103162, doi: https://doi.org/10.1016/j.jobe.2021.103162.

[2] V. Bernardo, R. Sousa, P. Candeias, A. Costa, and A. Campos Costa, "Historic appraisal review and geometric characterization of old masonry buildings in Lisbon for seismic risk assessment," *International Journal of Architectural Heritage*, vol. 16, no. 12, pp. 1921–1941, 2022, doi: https://doi.org/10.1080/15583058.2021.1918287.

[3] ISNA, "10 million buildings in Iran do not have skeletons: concern about the large number of unsustainable buildings," (2020, Jul. 24). [Online]. Available: https://www.isna.ir/news/99050301620.

[4] "Design and Construction of Masonry buildings, (part 8)," Ministry of Housing and Urban Development, Tehran, Iran, 2019 (in Persian).

[5] S. Motaghed, A. Nakhlian, L. Emadali, N. Eftekhari, and H. Mahmoudian, "Seismic hazard assessment using arithmetic-weighted overlay method based on earthquake potential index (EPI), the southwestern Iran," *Iranian Journal of Remote Sensing & GIS*, 2023, (in Persian), doi: https://doi.org/10.48308/gisj.2023.229646.1133.

[6] M. Abbasi Kia, M. Nadjafi, and A. Nadjafi, "Safety assessment of people in public building fire incidents using harmony search algorithm," *International Journal of Reliability, Risk and Safety: Theory and Application*, vol. 5, no. 2, pp. 33–40, 2022, https://doi.org/10.30699/IJRRS.5.2.4.

[7] M. H. Moghimi Esfandabadi, A. Esmaeili, and K. Karbasishargh, "Optimizing performance through retrofitting: strategies for effectiveness, defence, and resiliency to enhance safety and reliability," International Journal of Reliability, Risk and Safety: Theory and Application, vol. 7, no. 1, pp. 83–92, 2024, doi: 10.22034/IJRRS.2024.7.1.10.

[8] H. Araghizadeh, M. Saghafi Nia, and V. Entezari, "Analyzing medical management in disasters: A Review of the Bam Earthquake experience," *Journal of Military Medicine*, vol. 5, no. 4, pp. 259-268., 2004. (in Persian)

[9] M. Nekoei-Moghadam, M. Amiresmaili, and Z. Aradoei, "Investigation of obstacles against effective crisis management in earthquake," *Journal of Acute Disease*, vol. 5, no. 2, pp. 91-95, 2016, doi: https://doi.org/10.1016/j.joad.2015.10.001.

[10] K. Ziari, R. Ziari, and S. Ziari, "A case study of the Bam earthquake to establish a pattern for earthquake management in Iran.," *Space Ontology International Journal*, vol. 4, no. 1, 2015, pp. 63-70, 2015.

[11] A. Mehrabi Moghadam, A. Yazdani, and S. Motaghed, "Considering the yielding displacement uncertainty in reliability of mid-rise RC structures," *Journal of Rehabilitation in Civil Engineering*, vol. 10, no. 3, pp. 141–157, 2022, doi: https://doi.org/10.22075/jrce.2021.19660.1376.

[12] Farideh Moradi Tayebi, Sasan Motaghed, and Rezvan Dastanian, "Nature evaluation and time series prediction of Tehran earthquakes," *Modares Civil Engineering Journal*, vol. 20, no. 3, pp. 147–160, 2020. (in Persian)

[13] S. Motaghed, A. Mehrabi Moghaddam, and N. Moayyeri, "Reliability of Iranian existing residential reinforced concrete structures in seismic events," *International Journal of Reliability, Risk and Safety: Theory and Application*, vol. 6, no. 2, pp. 55–64, 2023, doi: https://doi.org/10.22034/ijrrs.2023.6.2.7

[14] S. Motaghed and A. R. Fakhriyat, "Modeling inelastic behavior of RC adhered shear walls in OpenSees," *Journal of Modeling in Engineering*, vol. 18, no. 63, pp. 15–25, 2021, (in Persian), doi: https://doi.org/10.22075/jme.2020.18042.1740.

[15] V. Barzian, S. Motaghed, A. Mehrabi Moghaddam, S. A. Asghari Pari, and L. Emadali, "Investigation the effect of structural parameters uncertainty on the response of incremental dynamic analysis of intermediate steel moment resisting frame structures," *Journal of Structural and Construction Engineering*, vol. 9, no. 10, pp. 175–195, 2022, (in Persian), doi: https://doi.org/10.22065/jsce.2022.311616.2612.

[16] A. Mehrabi-Moghaddam, S. Motaghed, A. Yazdani, and A. Mehrabi-Moghaddam, "Seismic assessment of collapse prevention limit-state of RC structures using numerical integration method," in *11th*

National Congress on Civil Engineering, Shiraz University, Shiraz, Iran, 2019.

[17] S. Motaghed and A. Khooshecharkh, "Probabilistic evaluation of the effects of concrete compression strength on the reinforced concrete building damageability," *European Journal of Scientific Research*, vol. 50, no. 2, pp. 202–207, 2011.

[18] S. Motaghed, M. S. Shahid Zadeh, A. Khooshecharkh, and M. Askari, "Implementation of AI for the prediction of failures of reinforced concrete frames," *International Journal of Reliability, Risk and Safety: Theory and Application*, vol. 5, no. 2, pp. 1–7, 2022, doi: https://doi.org/10.30699/IJRRS.5.2.1.

[19] S. Yaghmaei, S. Motaghed, A. Khooshecharrkh, "Correlation study between ground motion characteristic and RC frames damageability with intermediate ductility in Iran," Asas Journal, vol. 13, no. 28, pp. 60-70, 2018. (in Persian)

[20] L. F. Restrepo-Velez, and G.Magenes, "Simplified procedure for the seismic risk assessment of unreinforced masonry buildings, "In *13th world conference on earthquake engineering*, Vancouver, Canada, 2004, Art. no. 2561.

[21] J. Snoj and M. Dolšek, "Pushover-based seismic risk assessment and loss estimation of masonry buildings," *Earthquake Engineering and Structural Dynamics*, vol. 49, no. 6, pp. 567–588, 2020, doi: https://doi.org/10.1002/eqe.3254.

[22] A. Nicknam, M. Khanzadi, S. Motaghed, and A. Yazdani, "Applying b-value variation to seismic hazard analysis using closed-form joint probability distribution," *Journal of Vibroengineering*, vol. 16, no. 3, pp. 1376-1386, 2014.

[23] M. Khanzadi, A. Nicknam, A. Yazdani, and S. Motaghed, "A Bayesian approach for seismic recurrence parameters estimation," *Journal of Vibroengineering*, vol. 16, no. 2, pp. 977-986, 2014.

[24] P. Croce, F. Landi, and P. Formichi, "Probabilistic seismic assessment of existing masonry buildings," *Buildings*, vol. 9, no. 12, p. 237, 2019. doi: https://doi.org/10.3390/buildings9120237.

[25] M. Erdik, "Earthquake risk assessment," *Bulletin of Earthquake Engineering*, vol. 15, no. 12, pp. 5055–5092, 2017, doi: https://doi.org/10.1007/s10518-017-0235-2.

[26] D. W. Jia and Z. Y. Wu, "Seismic risk analysis based on imprecise distribution and failure probability function under multidimensional limit state," *Structures*, vol. 50, pp. 963–977, 2023, doi: https://doi.org/10.1016/j.istruc.2023.02.036.

[27] F. C. Ponzo et al., "Advanced modelling and risk analysis of RC buildings with sliding isolation systems designed by the Italian seismic code," *Applied Sciences*, vol. 11, no. 4, p. 1938, 2021, doi: https://doi.org/10.3390/app11041938.

[28] M. Ezzeldin, L. Wiebe, and W. El-Dakhakhni, "System-level seismic risk assessment methodology: Application to reinforced masonry buildings with boundary elements," *Journal of Structural Engineering*, vol. 143, no. 9, pp. 04017084, 2017.doi: https://doi.org/10.1061/(ASCE)ST.1943-541X.0001815

[29] M. D'Amato, R. Laguardia, G. Di Trocchio, M. Coltellacci, and R. Gigliotti, "Seismic risk assessment for masonry buildings typologies from L'Aquila 2009 earthquake damage data," *Journal of Earthquake Engineering*, vol. 26, no. 9, pp. 4545-4579, 2022, doi: https://doi.org/10.1080/13632469.2020.1835750.

[30] M. Nastev, "Adapting Hazus for seismic risk assessment in Canada," *Canadian Geotechnical Journal*, vol. 51, no. 2, pp. 217–222, 2014. doi: https://doi.org/10.1139/cgj-2013-0080.

[31] S. Mangalathu, "Performance based grouping and fragility analysis of box-girder bridges in California," Ph.D. dissertation, School of Civil and Environmental Engineering, Georgia Institute of Technology, Atlanta, USA, 2017.

[32] A. Badawy, I. Korrat, M. El-Hadidy, and H. Gaber, "Probabilistic earthquake hazard analysis for Cairo, Egypt," *Journal of Seismology*, vol. 20, pp. 449-461, 2016.

[33] S. Motaghed, M. Mohammadi, N. Eftekhari, and M. khazaee, "SCP parameters estimation for catalogs with uncertain seismic magnitude values," *Acta Geophysica*, 2024, doi: https://doi.org/10.1007/s11600-024-01404-5.

[34] A. Yazdani, A. Nicknam, M. Khanzadi, and S. Motaghed, "An Artificial statistical method to estimate seismicity parameter from incomplete earthquake catalogs, a case study in metropolitan Tehran, Iran," *Scientia Iranica*, vol. 22, no. 2, pp. 400-409, 2015.

[35] S. Motaghed, M. Khazaee, and M. Mohammadi, "The b-value estimation based on the artificial statistical method for Iran Kope-Dagh seismic province," Arabian Journal of Geosciences, vol. 14, no. 15, 2021, Art. no. 1461, doi: https://doi.org/10.1007/s12517-021-07970-y.

[36] S. Motaghed, M. Khazaee, N. Eftekhari, and M. Mohammadi, "A non-extensive approach to probabilistic seismic hazard analysis," *Natural Hazards and Earth System Sciences*, vol. 23, no. 3,

pp. 1117–1124, 2023, doi: https://doi.org/10.5194/nhess-23-1117-2023.

[37] K. K. S. Thingbaijam *et al.*, "Characteristic versus Gutenberg–Richter nucleation-based magnitude–frequency distributions in the New Zealand National Seismic Hazard Model 2022," *Seismological Research Letters*, vol. 95, no. 1, pp. 226-238, 2023, doi: https://doi.org/10.1785/0220230220.

[38] "Seismic evaluation and retrofit of concrete buildings," Applied Technology Council, California, USA, Rep. SSC 96-01: ATC-40, 1, 1996.

[39] "Earthquake model, Hazus–MH 2.1 technical manual," Federal Emergency Management Agency, Washington, USA, 2012.

[40] Z. Karim Zadeh, M. Ghafory-Ashtiany, A. Kalantari, and S. Shokuhirad, "Development of analytical seismic fragility functions for the common buildings in Iran," *Bulletin of Earthquake Engineering*, vol. 20, no. 11, pp. 5905–5942, 2022, doi: https://doi.org/10.1007/s10518-022-01411-1.

[41] "Instruction for Seismic Rehabilitation of Existing Buildings," Vice Presidency for Strategic Planning and Supervision, no. 92/131010, Tehran, Iran, 2014. (in Persian)

[42] H. Ghasemi, M. Zare, Y. Fukushima, and K. Koketsu, "An empirical spectral ground-motion model for Iran," *Journal of Seismology*, vol. 13, no. 4, pp. 499–515, 2008, doi: https://doi.org/10.1007/s10950-008-9143-x.

[43] S. Motaghed and A. Fakhriyat, "A reliable method for determining the tapered minimum magnitude in a probabilistic seismic hazard analysis," *International Journal of Reliability, Risk and Safety: Theory and Application*, vol. 5, no. 2, pp. 89–95, 2023, doi: https://doi.org/10.30699/ijrrs.5.2.9.

[44] S. Akkar and Z. Cagnan, "A Local Ground-Motion Predictive Model for Turkey, and Its Comparison with Other Regional and Global Ground-Motion Models," *Bulletin of the Seismological Society of America*, vol. 100, no. 6, pp. 2978–2995, 2010, doi: https://doi.org/10.1785/0120090367.

[45] S. Akkar, M. A. Sandıkkaya, and J. J. Bommer, "Empirical ground-motion models for point- and extended-source crustal earthquake scenarios in Europe and the Middle East," *Bulletin of Earthquake Engineering*, vol. 12, no. 1, pp. 359–387, 2013, doi: https://doi.org/10.1007/s10518-013-9461-4.

[46] B. J. Chiou and R. R. Youngs, "An NGA model for the average horizontal component of peak ground motion and response spectra," *Earthquake Spectra*, vol. 24, no. 1, pp. 173–215, 2008, doi: https://doi.org/10.1193/1.2894832.

[47] J. X. Zhao, "Attenuation Relations of strong ground motion in Japan using site classification based on predominant period," *Bulletin of the Seismological Society of America*, vol. 96, no. 3, pp. 898–913, 2006, doi: https://doi.org/10.1785/0120050122.

[48] Z. Fanni and A. Roshan, "Location of fire stations with passive defense approach Case study: Behbahan City," *Scientific- Research Quarterly of Geographical Data (SEPEHR)*, vol. 26, no. 101, pp. 81-92, 2017, doi: https://doi.org/10.22131/sepehr.2017.25728.

[49] Z. G. Rahmat *et al.*, "Landfill site selection using GIS and AHP: a case study: Behbahan, Iran," *KSCE Journal of Civil Engineering*, vol. 21, no. 1, pp. 111-118, 2017, doi: https://doi.org/10.1007/s12205-016-0296-9.

[50] M. Ghouchani, M. Taji, and M. Darbaniyan, "Evaluation of the effective factors on increasing the risk of damages to urban buildings in post-earthquake fire crisis by AHP method," (in eng), *Disaster Prevention and Management Knowledge*, Research vol. 9, no. 3, pp. 293-306, 2019, (in Persian).